

Article

Optimizing PCM Integrated Wall and Roof for Energy Saving in Building under Various Climatic Conditions of Mediterranean Region

Sana Dardouri ¹, Ekrem Tunçbilek ^{2,3}, Othmen Khaldi ⁴, Müslüm Arıcı ^{2,3,*}  and Jalila Sghaier ¹

¹ Research Laboratory of Thermal and Thermodynamic of Industrial Processes (LRTTPI), National Engineering School of Monastir, University of Monastir, Monastir 5000, Tunisia

² Mechanical Engineering Department, Engineering Faculty, Kocaeli University, Umuttepe Campus, Kocaeli 41001, Turkey

³ International Joint Laboratory on Low-Carbon and New-Energy Nexus Research and Development, Kocaeli University, Kocaeli 41001, Turkey

⁴ Laboratory of Materials Organization and Properties LMOP (LR99ES17), University of Tunis El Manar, Tunis 2092, Tunisia

* Correspondence: muslumarici@gmail.com

Abstract: Energy conservation in buildings has been the focus of many studies since nearly one-third of global energy consumption is due to buildings. Phase change material (PCM) technology promises to be an attractive solution for energy saving in buildings since it is a passive and effective technology, as demonstrated in the literature. Therefore, this study focuses on the energy-saving performance of PCM-integrated buildings located in a Mediterranean climate to reveal their energy-saving potential. PCM is integrated both in external or internal south walls and roofs of buildings under four different climatic conditions. EnergyPlus, which is a well-known building simulation software, is adopted for building thermal analyses. The effects of melting temperature, location of PCM layer in the wall, thickness of PCM layer, type of envelope (wall or roof), and PCM double-layer system in the wall are investigated. The corresponding energy savings and CO₂ emission reductions are obtained for the considered cases. The results showed that up to 41.6% reduction in energy demand can be obtained depending on the PCM application. Besides, PCM with a low melting temperature (21 °C) favored heating energy savings, while PCM with a high melting temperature (29 °C) favored cooling energy savings. Moreover, the double-layer PCM system provided higher energy savings than the single-layer PCM system, especially in warm and arid regions (Sousse and Tozeur).

Keywords: phase change materials; building performance; climatic condition; PCM melting temperature; CO₂ reduction; PCM double layer



Citation: Dardouri, S.; Tunçbilek, E.; Khaldi, O.; Arıcı, M.; Sghaier, J. Optimizing PCM Integrated Wall and Roof for Energy Saving in Building under Various Climatic Conditions of Mediterranean Region. *Buildings* **2023**, *13*, 806. <https://doi.org/10.3390/buildings13030806>

Academic Editor: Cinzia Buratti

Received: 12 January 2023

Revised: 6 March 2023

Accepted: 11 March 2023

Published: 18 March 2023



Copyright: © 2023 by the authors. Licensee MDPI, Basel, Switzerland. This article is an open access article distributed under the terms and conditions of the Creative Commons Attribution (CC BY) license (<https://creativecommons.org/licenses/by/4.0/>).

1. Introduction

Global energy consumption is gradually increasing with the continuous development of technology, although considerable efforts have been put into increasing energy efficiency and thereby decreasing energy demand. Considering the fact that most fossil fuels are used as primary energy sources to supply energy to the energy networks, an inevitable shortage of these sources is obvious in the upcoming years. In addition to that, the high amount of greenhouse gas emitted in the process of generating energy is another important factor that has to be focused on when it is considered that these emissions lead to the greenhouse gas effect. In this context, the development of new energy sources is a major issue for the scientific community, and several works and research studies have been carried out in this field with the aim to improve energy efficiency, gain energy saving, and limit greenhouse gas emissions [1–3].

In Tunisia, the energy consumed in the building sector is approximately 36% of the national total energy consumption (Figure 1). Obviously, this percentage tends to increase

in the upcoming years considering the technological development, rising population, and increasing comfort expectations of people [4,5]. Transportation and industry followed the building sector's energy consumption with 31% and 27% shares, respectively, in the national final energy consumption. The building sector indeed has great potential for energy savings since a majority of the buildings lack even proper thermal insulation, and previous works in the literature showed that energy saving in buildings can reach considerable rates [6–8]. In addition, the Social Commission for Western Asia (ECWAS), the German Development Agency (GIZ), and the UN's Economic and Social Council have recently evaluated the energy situation of buildings in Tunisia [9]. The study evaluated the diverse energy consumption items (air conditioning, heating, lighting, cooling, office equipment, etc.) in public, private, and office buildings in detail. These findings represented a database of electricity consumption estimations in Tunisia's buildings. For instance, in 2017, the total energy consumption for the residential sector reached 5176.2 GWh (13.07 kWh/m² over the year), a radical increase of 27% as compared to the energy consumption observed in 2014. Among the evaluated parameters, cooling is classified as the first on the list (30.3% of the total), followed by air conditioning (22.2% against 3.4% in 2004) and television sets (17.2% against 21.16% in 2004) [9].

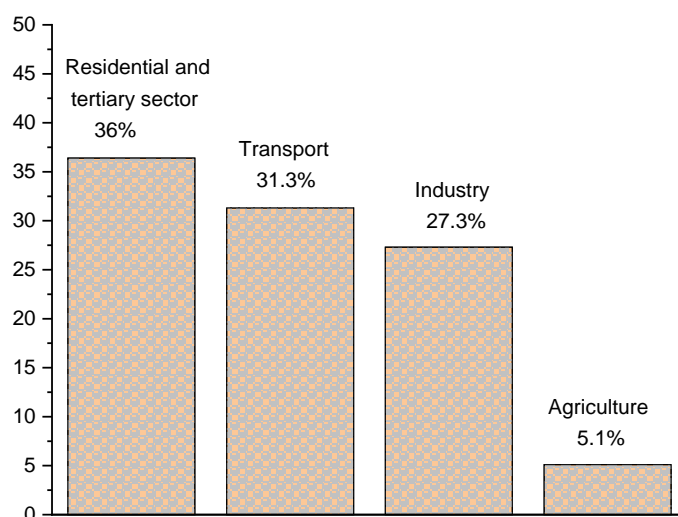


Figure 1. Final energy consumption in 2020 with respect to sector in Tunisia [9].

Thus, it is crucial to decrease energy consumption in the residential sector by improving both energy efficiency as well as saving measures. In this context, phase change thermal energy storage represents an innovative and promising way for energy storage technology. This can be realized particularly with phase change materials (PCM), which have the potential to store latent heat in materials such as paraffin waxes, eutectics, and salt hydrates. The application of PCMs in building envelopes can reduce space heating/cooling energy demand and be considered a promising passive cooling technology in buildings that have poor energy efficiency and thermal comfort [10].

Recently, a good amount of research has been dedicated to the utilization of PCM as well as nano-enhanced PCM applications in buildings [11–16]. It is obvious from the literature review that the PCM technique is successfully integrated into the walls [11,13], windows [14,15], floors [16,17], and roofs [18,19] to reduce the energy requirement of the buildings [20]. For instance, Chelliah et al. [13] studied the energy-saving potential of air-conditioning by evaluating PCM-filled terracotta bricks in the external walls. They reported that there is an optimum PCM with a certain melting temperature and that up to EUR 74 in cost savings can be achieved. Hamidi et al. [21] integrated PCM into hollow brick walls and indicated that the percentage of energy saved is about 56% in the northeast Mediterranean zone, while no energy-saving effect is observed for the southeast zone. Besides, for the northeast zone, a 26 °C optimum melting temperature for PCM is suggested as it gives the

best thermal performance. Kenzhekhanov et al. [22] demonstrated the promising effect of the PCM location as well as the PCM amount on the energy savings and discomfort hours of a building located in a subarctic climate. They reported that increasing the thickness and amount of PCM in the layer promotes more energy savings. Besides, up to 10,000 kWh and 500 h of annual energy savings and discomfort hour reductions are respectively achieved with PCM integration.

Applications related to PCM building and analysis of energy efficiency, energy saving, or thermal comfort are simulated and analyzed in several works. However, studies on the position, thickness, and type of PCM in the envelope should be performed and detailed carefully prior to the application of innovative materials to buildings [23,24]. For example, Hu [25] studied thermal and building envelope responses to light under several climate situations. The total energy consumed was reduced by 19% for the roof with a thermochromic coating (TC roof)—PCM, which in turn reduced CO₂ emissions by 5%. So, as the PCM roof thickness increases, the energy savings increase and reach 29%, while CO₂ emission reductions become 8%. Additionally, as mentioned in [26], PCM with a melting temperature close to 24 °C was successfully integrated into the building wall to maintain the indoor temperature of the building. This work shows that comfortable temperatures can be maintained for the whole year without the contribution of any mechanical air-conditioning system. These results agree well with several numerical investigations in Morocco, in which the improvement of the thermal efficiency of PCM-integrated double external walls was considered [27]. A previous work by Hagenau [28] investigated the role of PCM and the related dynamic energy in order to evaluate building envelope performance under various Danish climate zones, and the researchers reported that energy savings in the range of 32–36% can be achieved. Considering the abovementioned works, it is important to note that using PCM in the walls and roofs increases the cost of construction. Therefore, it is obvious to search for the most favorable location for PCM integration to gain the best possible energy conservation. In this context, a dynamic model based on hysteresis was used to find the best location of PCM thickness in the wall and roof, as well as its appropriate position for heat flux reduction [29].

From the literature review, it is clear that PCM integration into the building's external walls promises to be a good candidate for energy saving. Besides, it is also known that melting temperature, location, and thickness of PCM are important parameters affecting TPCM energy-saving performance. The optimum melting temperature and location can be different depending on the outdoor boundary conditions. Therefore, in this study, an optimization of PCM properties is conducted to gain the highest possible energy saving from PCM application to the building's external envelope. In this respect, different PCM melting temperatures, PCM locations (in the wall and roof), and PCM thicknesses are studied based on thermal analyses. Furthermore, these thermal analyses are conducted for four different climatic regions of Tunisia so an effective guideline can be presented with relevant findings. The main targets of this study can be listed as (i) exploring the effect of PCM features (melting temperature, location, and thickness) on energy saving; (ii) revealing the energy saving potentials by utilizing PCM in different climatic regions of Tunisia; (iii) the impact of using double-layer PCM in the external wall on the energy saving; and (iv) providing a practical guideline that can be valid for different climatic regions of Tunisia for building envelope applications of PCM.

2. Methodology

2.1. Model Description

A building with standard wall, roof, and floor structures is considered to be used in thermal analyses. The building is one story, has two standard-sized windows on the south side, and the window-to-wall ratio on that side is approximately 40%. The floor area is 72 m², and the building has a flat roof. The building is conditioned by using an air-cooled heat pump for both heating and cooling purposes. In order to ensure thermal comfort conditions inside the building, the heating and cooling set temperatures are taken

as 21 °C and 24 °C, respectively. Besides, the heating and cooling setback temperatures are considered for preventing excessive cooling (in winter) and heating (in summer) when the building is not occupied.

2.2. Numerical Simulation

In this work, Design Builder is employed as the graphical interface for EnergyPlus software. EnergyPlus is a software that is capable of performing building thermal simulation, and its development was funded by the U.S. Department of Energy's (DOE) Building Technologies Office (BTO). Based on a definition of a building in terms of the physical design of the building, associated mechanical systems, etc., the software simulates the outdoor and indoor conditions to calculate the heating and cooling loads required to maintain thermal control setpoints. EnergyPlus includes several modules to estimate building energy requirements. It does not have its own graphical user interface, but several interfaces are available for inputting data and processing simulation results (Figure 2).

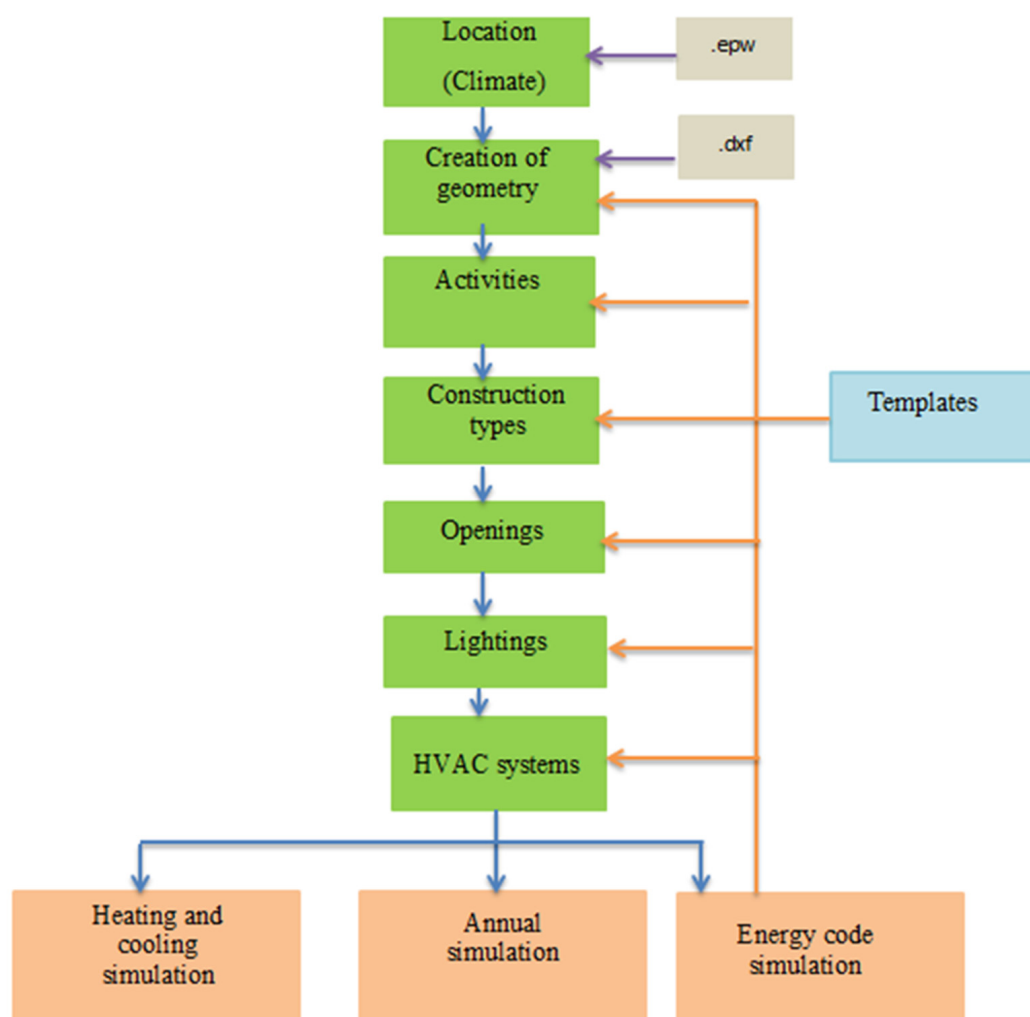


Figure 2. EnergyPlus program flow chart.

The EnergyPlus PCM model based on the one-dimensional conduction finite-difference (CondFD), which was subject to various verification studies and has been validated by several researchers [30–34], is adapted as the solution algorithm. This algorithm gives the user the possibility to choose between an implicit finite difference scheme and the Crank–Nicholson method. In this study, an implicit finite difference scheme coupled with the enthalpy–temperature equation is used to evaluate phase change and find the temperature field (Equations (1) and (3)). All elements were discretized using a node

spacing Δx , which depends on the time step (Δt), the space discretization constant (c), and the thermal diffusivity of the material (α) (Equation (2)).

$$\rho C_p \Delta x \frac{T_j^{n+1} - T_j^n}{\Delta t} = \left(\frac{\lambda_{j+1}^{n+1} + \lambda_j^{n+1}}{2} \right) \left(\frac{T_{j+1}^{n+1} - T_j^{n+1}}{\Delta x} \right) + \left(\frac{\lambda_{j-1}^{n+1} + \lambda_j^{n+1}}{2} \right) \left(\frac{T_{j-1}^{n+1} - T_j^{n+1}}{\Delta x} \right) \quad (1)$$

$$\Delta x = \sqrt{c\alpha\Delta t} \quad (2)$$

$$C_p = \frac{h_j^{new} - h_j^{old}}{T_j^{new} - T_j^{old}} \quad \text{where } h = h(T) \quad (3)$$

where T stands for temperature and λ stands for thermal conductivity of the wall material. Besides, ρ and C_p represent the density and specific heat capacity of the material, respectively. Enthalpy is denoted by h . In the thermal analyses, 60 time steps per hour ($\Delta t = 1$ min) are taken, while the space discretization constant (c) in the node spacing equation is taken as 0.5.

2.3. Climatic Conditions

Climatic conditions have a great impact on building thermal efficiency and performance. The scope is focused on the region of Tunisia, due to its strategic location. As shown in Figure 3, the climate of Tunisia is divided into five climatic zones, namely, arid, upper humid, Saharian, lower semi-arid, and lower humid. According to the Köppen–Geiger classification [35], a great difference between the north and the rest of the country occurs due to the chain of the Tunisian ridge, which separates the zones subjected to the Mediterranean climate as humid (for Bizerte and Tabarka), lower semi-arid (for Sousse) and the hot desert climate typical of the Sahara (for Tozeur) (Table 1). The weather data for each city are exported to the EnergyPlus climate file database. The geographic and meteorological data of these regions, as well as the city description, are given in Table 1.

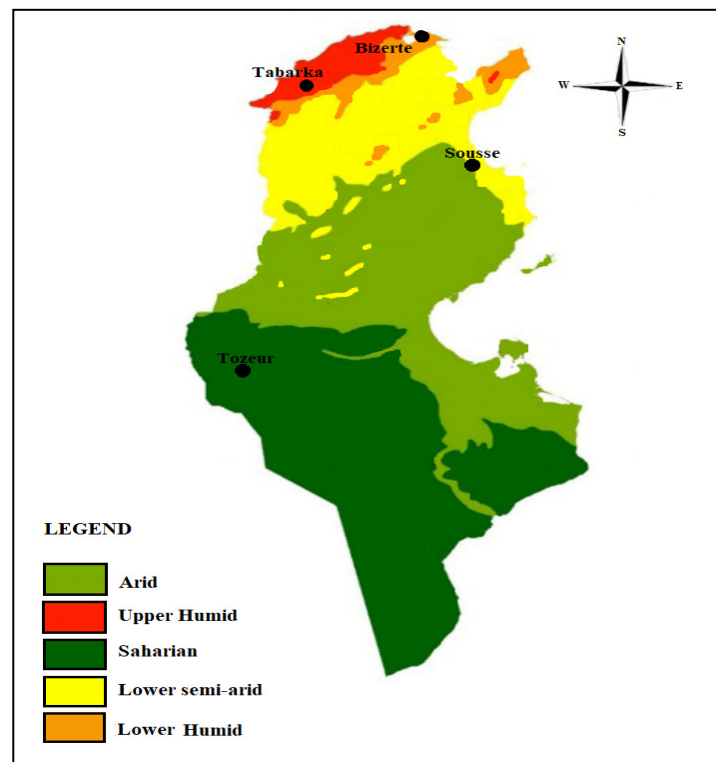


Figure 3. Map of climatic zones in Tunisia.

Table 1. Considered cities located in different climatic zones.

Region (City)	Climate Classification	Latitude	Longitude	Elevation [m]
Sousse	Lower semi-arid	35°40' N	10°45' E	24
Bizerte	Lower humid	37°15' N	9°48' E	5
Tabarka	Upper humid	36°57' N	8°45' E	4.69
Tozeur	Saharian	33°55' N	8°06' E	42

With a cold and rainy winter season, the heating loads are dominant in Tabarka, and snow is possible during this period of the year with an average temperature of 7.4 °C. However, summer is usually hot and dry, with an average temperature of 28.2 °C. Besides, Sousse is characterized by a hot, semi-arid climate, which makes it an all-season resort with hot, dry summers and warm, wet, mild winters. Bizerte is characterized by a warm-summer Mediterranean climate, with mild and rainy winters. Summers are hot and dry, and together with the Mediterranean Sea, summers are cooler and more humid than in the interior of Tunisia. For Bizerte and Sousse, both heating and cooling are required. Conversely, Tozeur suffers from hot desert climate conditions. Summer is exceptionally hot, with daily temperatures frequently exceeding 45 °C in the shadows, and the sirocco (Mediterranean wind) can force temperatures to exceed 50 °C. In winter, it can sometimes turn freezing at night, and just before sunrise, the temperature drops below 0 °C. Depending on the incident solar radiation, the highest solar radiation is observed in April, May, June, July, and August in Sousse, Tozeur, Bizerte, and Tabarka, respectively, which in turn improves the solar heat gain in buildings through the building envelope.

The outdoor temperatures (T_{air}) as well as the wind speed (w) are given in Ref. [36], while the collected solar radiation data are available in Ref. [37]. Therefore, the corresponding annual climate data are collected from these sources and depicted in Figure 4.

2.4. PCM Properties

In this work, the Infinite RTM PCMs were chosen, which are used in diverse commercial applications such as energy storage with diverse melting temperatures of 18, 21, 23, 25, and 29 °C, referred to as PCM18, PCM21, PCM23, PCM25, and PCM29, respectively. The thermophysical properties of the Infinite RTM PCMs are given in Table 2.

Table 2. Thermophysical properties of PCM.

	PCM18	PCM21	PCM23	PCM25	PCM29
Latent heat during the entire phase change (kJ/kg)	200	200	200	200	200
Peak melting temperature for melting curve (°C)	19	22	24	26	30
Peak melting temperature for freezing curve (°C)	17	20	22	24	28
Liquid state thermal conductivity (W/(mK))	0.54	0.54	0.54	0.54	0.54
Solid state thermal conductivity (W/(mK))	1.09	1.09	1.09	1.09	1.09
Liquid state density (kg/m ³)	1540	1540	1540	1540	1540
Solid state density (kg/m ³)	1540	1540	1540	1540	1540
Liquid state specific heat (J/(kgK))	3140	3140	3140	3140	3140
Solid state specific heat (J/(kgK))	3140	3140	3140	3140	3140

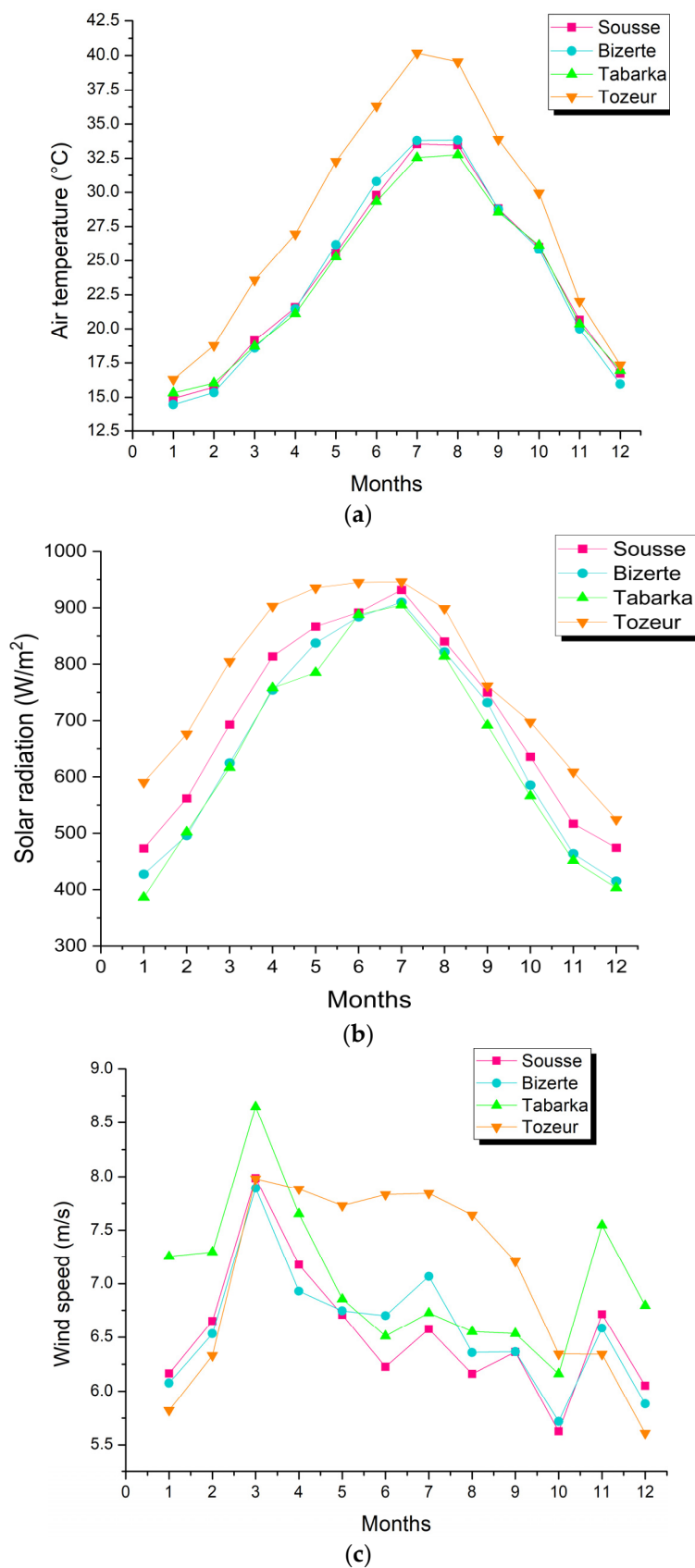


Figure 4. Climatic data (a) air temperature, (b) solar radiation, and (c) wind speed.

2.5. Wall and Roof Structure in the Building

In Tunisia, the brick wall is the conventional structure for residential building construction [37]. Here, the external building wall without PCM (control wall) is composed of three layers: plaster coating, brick, and cement (Figure 5a). On the building roof, four layers were considered: cement, concrete, reinforced concrete, and plaster coating (Figure 5b). Two different configurations were considered for PCM integration into the control wall: (i) PCM located in the outside of the wall (Case 1, Figure 5c) and (ii) PCM located in the inside of the wall (Case 2, Figure 5c). It should be noted that PCM is employed in the wall as an extra layer. The PCM layer thickness is varied between $e = 10$ mm and 30 mm for these configurations. The thermal performances of these materials, as described in Table 3, were also taken into account in the modeling process.

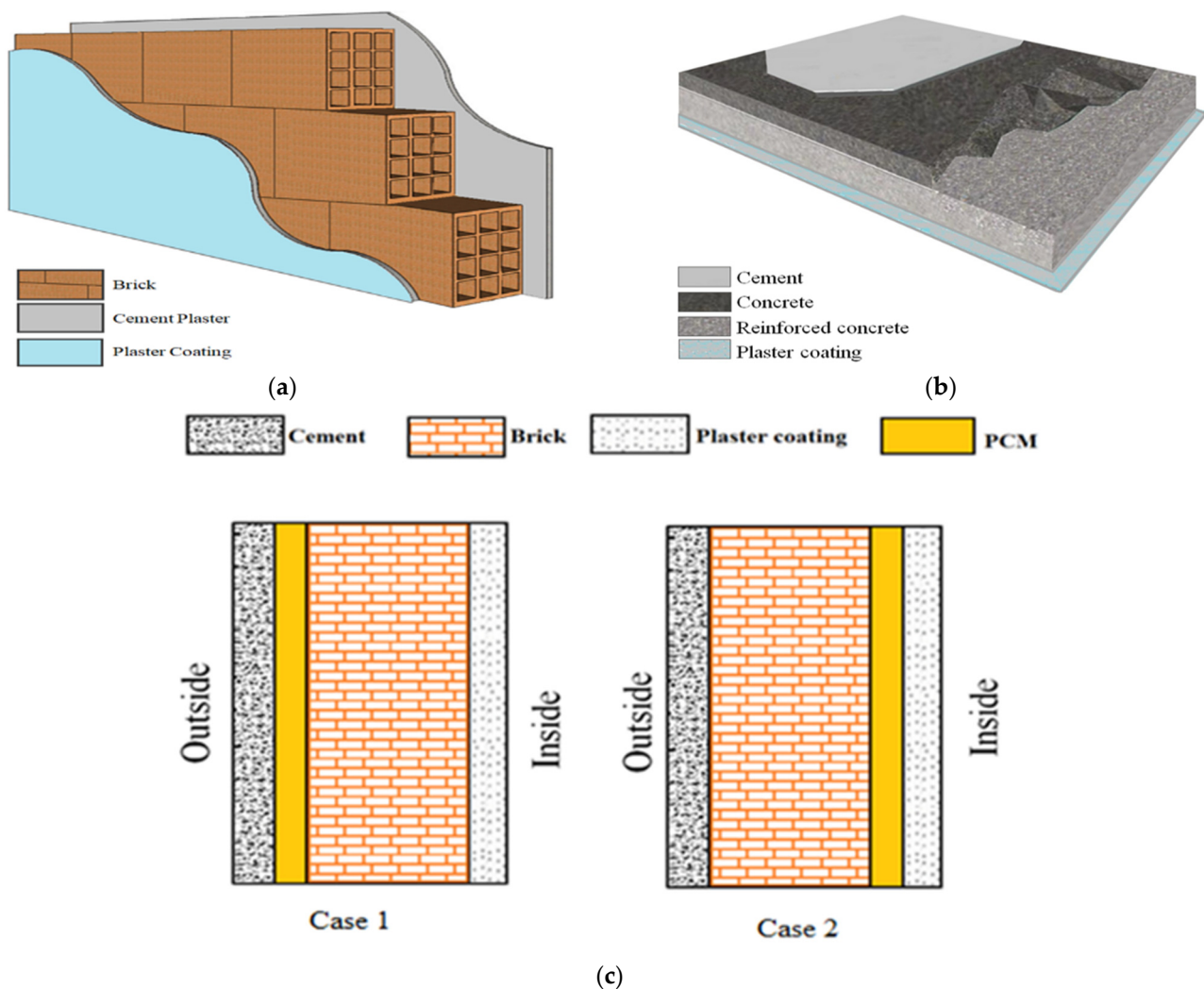


Figure 5. Schematic representation of (a) external wall, (b) roof, and (c) PCM integration.

To evaluate the effectiveness of the implementation of the PCM layer in the building's external envelope, two indicators are used:

- (i) Energy savings: It gives the total decrease in energy consumption resulting from the integration of PCMs.

This can be deduced from Equations (4) and (5) for both heating and cooling energy savings, respectively.

$$E_{\text{saving,heating}} = E_{\text{heating consumption, without PCM}} - E_{\text{heating consumption, with PCM}} \quad (4)$$

$$E_{\text{saving,cooling}} = E_{\text{cooling consumption, without PCM}} - E_{\text{cooling consumption, with PCM}} \quad (5)$$

- (ii) The annual percentage of heating and cooling energy consumption reduction due to the PCM integration, the rate R (in %), is given by the following equation:

$$R (\%) = \frac{E_{\text{saving}}}{E_{\text{consumption, without PCM}}} * 100 \quad (6)$$

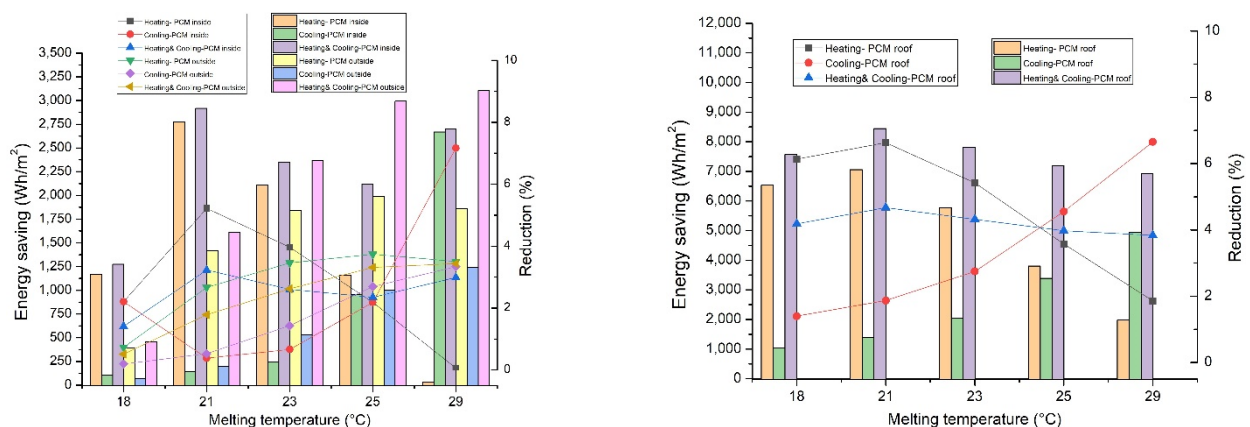
Table 3. Thermal properties of materials.

	k (W/mK)	ρ (kg/m ³)	C_p (J/kgK)	e (m)
Brick	0.72	1920	840	0.20
Cement	1.4	2200	940	0.025
Plaster coating	1.2	1800	840	0.015
Concrete	1.4	2100	840	0.1
Reinforced concrete	2.3	2300	1000	0.15

3. Results and Discussion

3.1. Effect of PCM Melting Temperature

The effect of PCM melting temperature on the total energy saving was evaluated by testing different phase transition temperatures ranging from 18 °C to 29 °C. The thickness of the PCM layer was taken as 10 mm, and the PCM was located both near the interior as well as near the exterior surface of the south wall to also reveal the impact of the PCM location on the melting temperature. The obtained results related to the parameters above are given in Figure 6. From the figures, it can be deduced that the PCM21 (i.e., PCM with a 21 °C melting temperature) provided the highest energy saving for Bizerte, Tabarka, and Tozeur, whereas the PCM29 showed the best performance for Sousse. The highest energy-saving amounts were also attained by locating the PCM layer near the interior surface rather than near the exterior, regardless of the city except for the Sousse region. The same finding, that the PCM layer near the indoor outperforms that near the outdoor, was also pointed out in the literature.



(a) Sousse

Figure 6. Cont.

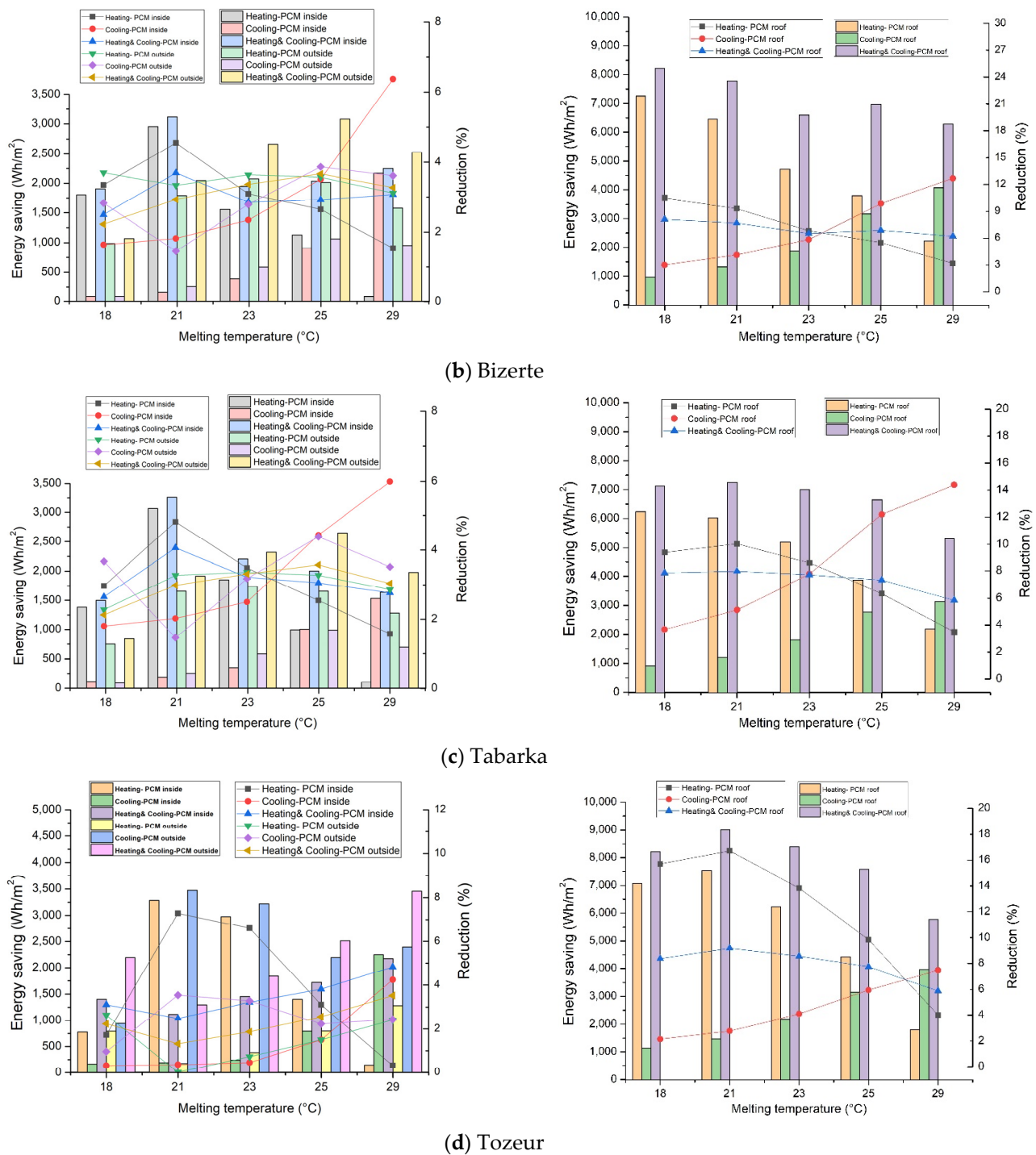


Figure 6. Effect of PCM melting temperature on energy saving and energy reduction.

Excluding the worst-case scenario for all the considered cities (PCM18), the total energy savings ranged from 3116.0 Wh/m² (PCM21) to 1946.0 Wh/m² (PCM23) for Bizerte, from 3259.9 Wh/m² (PCM21) to 1639.9 Wh/m² (PCM29) for Tabarka, and from 3474.21 Wh/m² (PCM21) to 2145.6 Wh/m² (PCM25) for Tozeur with PCM located near the interior. As previously mentioned, the optimum melting temperature for PCM-integrated walls near the indoor environment was found to be 21 °C, except for the Sousse. A total energy saving of 3104.7 Wh/m² can be attained with PCM29 located near the exterior surface of the wall under Sousse climatic conditions, indicating that the melting temperature should be 29 °C. It was noted that the PCM location inside the wall affected the optimum melting

temperature for the PCM. For instance, the optimum melting temperature for all cities was found to be 29 °C when the PCM was located near the interior surface of the wall for the cooling energy. Overall, the PCM location inside the wall and the climatic conditions of the region significantly affected the thermal performance of the PCM application. It can be deduced from the results that the optimum melting temperature was close to the setpoint of the room [38]. For example, the melting temperature was equal to 21 °C for the heating load in each city. On the contrary, the optimum melting temperature was equal to 29 °C for cooling loads in all cities. Moreover, it was shown that higher energy-saving amounts can be attained in high-amplitude regions. When the PCM layer is located near the exterior or interior roof surface, the optimum melting temperature is always equal to 21 °C for all regions except for Bizerte (found at 18 °C), which is located in a relatively cold region. In summary, it can be concluded that when modeling an implementation of PCM building technology, one should consider geographical and climatic factors such as temperature, wind profile, and solar irradiance [39].

3.2. Effect of Building Envelope Type and PCM Location

Utilization of PCM in different building envelope types was studied by integrating PCM in the roof, external or internal wall, and wall-roof of the building. In the wall-roof configuration, PCM21 is located in the interior surface of the wall, except in the Sousse region, where PCM29 is placed on the exterior surface of the wall. Moreover, PCM location was found to be an important parameter in the literature; therefore, two different locations, namely near the interior and near the exterior, were tested. The overall effect of these variables on the energy saving in heating, cooling, and total energy demand was then analyzed using the optimum melting temperature of PCM for each city. The obtained results related to optimal envelope type, location, and configuration are given in Figure 7.

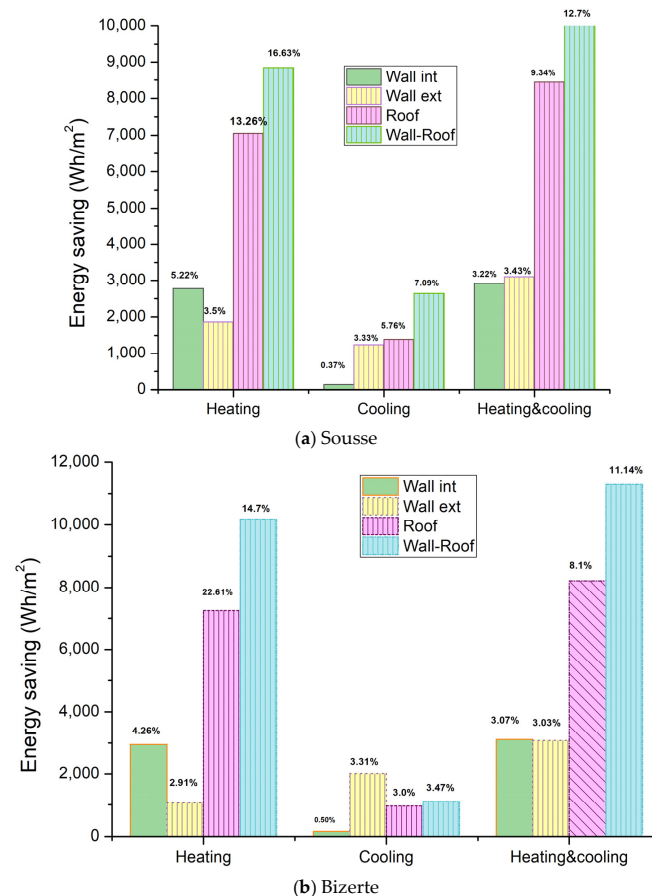


Figure 7. Cont.

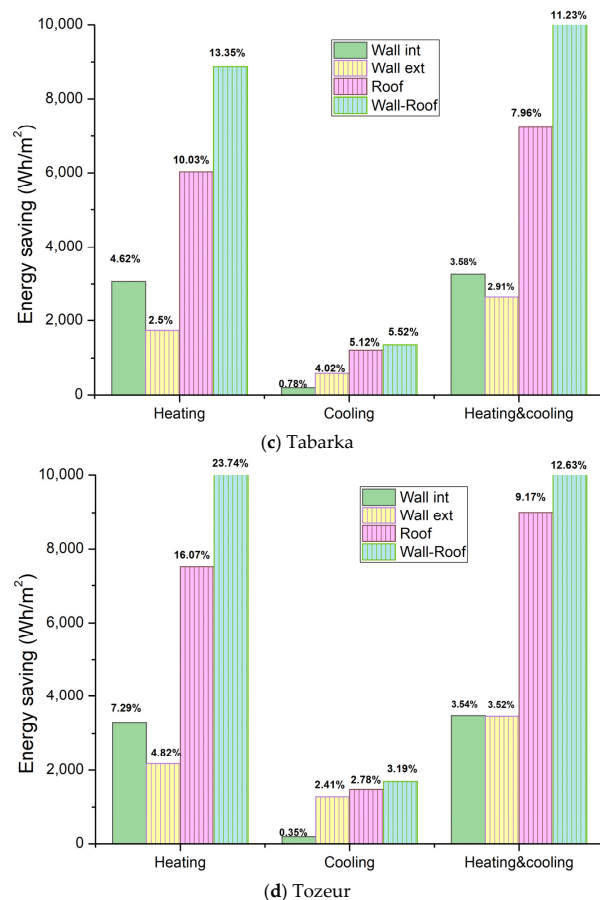


Figure 7. Effect of envelope type and PCM location on the energy saving.

It can be seen from the given figure that the utilization of PCM provided significant energy savings both in heating and cooling applications for all of the considered cities, regardless of the PCM location (Wall int and Wall ext) as well as building envelope type (wall, roof, or wall-roof). The interior location for PCM21 was found to be more beneficial in terms of energy saving compared to the exterior location for the heating period. However, on the contrary, the exterior location saved more energy than the interior location for the cooling period. As compared to the traditional building envelopes, the reduction in the heating load reached 16.6%, 23.7%, 14.7%, and 13.6% in Sousse, Tozeur, Bizerte, and Tabarka, respectively, by implementing PCM21 in a wall-roof configuration. Although considerable reductions in energy consumption for cooling were achieved, these savings are marginal compared to the amount saved in heating energy. Using PCM in both the internal wall (with higher energy saving) and roof (wall-roof configuration) provided the highest energy saving amount irrespective of the city, i.e., climatic region. The least-efficient scenario was attained when the PCM was integrated into the exterior wall in the heating period and into the interior wall during the cooling period. The corresponding total energy reduction percentages for PCM integrated roofs are 9.34%, 9.2%, 8.1%, and 7.9% in Sousse, Tozeur, Bizerte, and Tabarka, respectively. In total, the PCM located near the interior (near the indoor) saved more energy than the PCM located near the exterior (near the outdoor) in all climatic regions except the Sousse region. This finding agrees with the findings reported in Refs. [40–42]. Consequently, approximately 12.4 kWh/m² energy savings were achieved for Tozeur (warm region) when the optimum configuration was applied, i.e., PCM integration in both wall and roof (wall-roof case).

3.3. Effect of PCM Layer Thickness

The impact of the PCM thickness on the energy-saving performance was investigated by analyzing different thicknesses, namely, 10 mm, 20 mm, 30 mm, and 40 mm. The optimized phase transition temperature of the PCM layer, i.e., the optimum PCM type, was used in the simulations. For heating, cooling, and heating and cooling, the PCM layer was tested in both types, near the interior surface of the wall and near the exterior surface of the roof. The results are given in Table 4. It is evident from the table that the total energy requirement (heating and cooling) is greater in the case of increasing the PCM layer thickness. This can be expected since a higher amount of latent heat can be stored due to the increased PCM amount [42]. Higher energy requirement reduction was achieved with a 40 mm PCM located in the roof and also in the wall. The heating and cooling energy needs were reduced by 26.7 kWh/m², 23.3 kWh/m², 21.6 kWh/m², and 30.8 kWh/m² with a 40 mm PCM located in the roof for the buildings in Sousse, Bizerte, Tabarka, and Tozeur, respectively. Following the PCM located in the roof, the best case was found for locating the PCM near the interior wall surface, regardless of the PCM layer thickness. These results also comply with the outcomes of the studies in the literature [38–44].

Table 4. Annual heating and cooling energy saving per 1 m² of three types of building envelopes and for five PCM layer thicknesses.

		e ₁ = 10 mm	e ₂ = 20 mm	e ₃ = 30 mm	e ₄ = 40 mm
		Heating (Wh/m ²)			
Sousse	PCM-wall	1862.87 (−3.50%)	3688.96 (−6.93%)	4834.89 (−9.09%)	5514.46 (−10.36%)
	PCM-roof	7056.94 (−13.26%)	13,703.54 (−25.76%)	19,543.38 (−36.74%)	21,476.14 (−40.37%)
	Cooling (Wh/m ²)				
	PCM-wall	1241.79 (−3.33%)	2105.36 (−5.65%)	2344.13 (−6.29%)	2330.63 (−6.26%)
	PCM-roof	1389.78 (−3.73%)	2689.36 (−7.22%)	3594.85 (−9.65%)	5257.56 (−14.12%)
		Heating and Cooling (Wh/m ²)			
Sousse	PCM-wall	3104.66 (−3.43%)	5794.32 (−6.40%)	7179.02 (−7.94%)	7845.09 (−8.67%)
	PCM-roof	8446.72 (−9.34%)	16,392.9 (−18.13%)	16,392.9 (−18.13%)	26,733.7 (−29.57%)
		Heating (Wh/m ²)			
Bizerte	PCM-wall	2953.44 (−4.26%)	4092.55 (−5.90%)	4565.82 (−6.59%)	4852.72 (−7.00%)
	PCM-roof	7253.05 (−10.47%)	12,206.94 (−17.62%)	16,656.06 (−24.04%)	18,763.45 (−27.08%)
	Cooling (Wh/m ²)				
	PCM-wall	162.6 (−0.50%)	299.2 (−0.93%)	387.45 (−1.20%)	425.04 (−1.32%)
	PCM-roof	963.84 (−3.00%)	2340.42 (−7.29%)	3102.68 (−9.67%)	4579.27 (−14.27%)
		Heating&Cooling (Wh/m ²)			
Bizerte	PCM-wall	3116.04 (−3.07%)	4391.75 (−4.33%)	4953.27 (−4.88%)	5277.76 (−5.20%)
	PCM-roof	8216.89 (−8.10%)	14,547.36 (−14.35%)	19,758.74 (−19.49%)	23,342.72 (−23.03%)

Table 4. Cont.

		$e_1 = 10 \text{ mm}$	$e_2 = 20 \text{ mm}$	$e_3 = 30 \text{ mm}$	$e_4 = 40 \text{ mm}$
		Heating (Wh/m ²)			
Tabarka	PCM-wall	3067.38 (−4.62%)	3997.52 (−6.02%)	4721.15 (−7.11%)	5494.2 (−8.28%)
	PCM-roof	6029.15 (−9.09%)	11,606.52 (−17.50%)	15,731.54 (−23.72%)	17,727.22 (−26.73%)
	Cooling (Wh/m ²)				
	PCM-wall	192.55 (−0.78%)	336.41 (−1.37%)	444.68 (−1.81%)	515.54 (−2.10%)
	PCM-roof	1212.54 (−4.94%)	1001.02 (−4.07%)	734.94 (−2.99%)	958.68 (−3.9%)
	Heating and Cooling (Wh/m ²)				
PCM-wall	3259.93 (−3.59%)	433.93 (−4.77%)	5165.83 (−5.68%)	6009.74 (−6.61%)	
PCM-roof	724,169 (−7.97%)	13,820.08 (−15.21%)	18,680.04 (−20.55%)	21,634.4 (−23.80%)	
		Heating (Wh/m ²)			
Tozeur	PCM-wall	3285.02 (−7.29%)	4414.55 (−9.80%)	5320.52 (−11.81%)	5860.36 (−13.01%)
	PCM-roof	7525.08 (−16.70%)	15,295.52 (−33.95%)	20,391.24 (−45.26%)	25,419.04 (−56.42%)
	Cooling (Wh/m ²)				
	PCM-wall	189.19 (−0.36%)	355.44 (−0.67%)	516.83 (−0.97%)	649.39 (−1.22%)
	PCM-roof	1478.44 (−2.79%)	2810.79 (−5.30%)	4370.75 (−8.24%)	5407.76 (−10.19%)
	Heating and Cooling (Wh/m ²)				
PCM-wall	3474.21 (−3.54%)	4769.99 (−4.86%)	5837.35 (−5.95%)	6509.75 (−6.64%)	
PCM-roof	9003.52 (−9.18%)	18,106.31 (−18.45%)	24,761.99 (−25.24%)	30,826.8 (−31.42%)	

3.4. Effect of Double-Layer PCMs

The double-PCM layer model was considered to benefit from the thermal properties of two PCMs at different locations with different melting temperatures. The model was formed by two PCMs with the same thickness as the PCM single layer. In order to analyze the efficiency of a double-PCM layer and energy saving, two configurations of a double-PCM layer were proposed in Figure 8. In Case 1, the first PCM layer was placed on the exterior surface with a different melting temperature, and the second was located in the interior surface of the wall with a fixed melting temperature (the optimum melting temperature is 21 °C) in all the cities. In Case 2, the first PCM layer (PCM1) represents the optimum melting temperature, allowing for more heating energy saving (21 °C), and the second PCM layer (PCM2) provides the PCM gives more reduction in cooling energy consumption. Based on the previous simulations, PCM21 is used as the first layer of the double-layer system due to the corresponding higher heating energy saving, while PCM29 and PCM25, which perform better cooling energy saving in warm and cold regions, respectively, are applied to the second layer. In Case 2, two double-PCM layer systems were considered: PCM21-PCM29 and PCM21-PCM25. The obtained results for the considered cases are given in Table 5. Accordingly, in Case 1, the PCM21-PCM29 double layers represent the best energy saving in warm regions (Sousse and Tozeur). Whereas, it does not apply to cold regions. The same results are obtained in Case 2, where an improvement in cooling and heating energy saving is achieved for the PCM21-PCM29 double layer for Sousse and Tozeur as well.

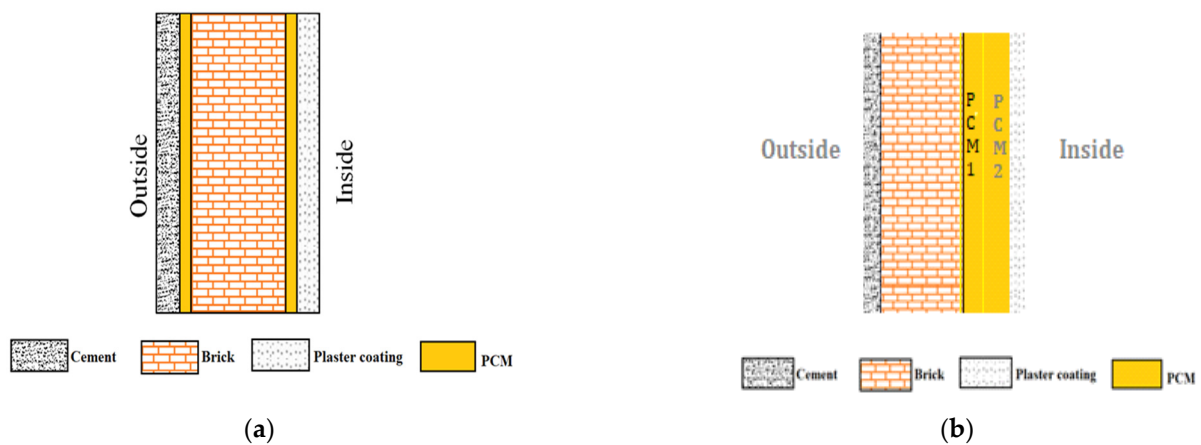


Figure 8. Schematic representation of double layer of PCM location in wall (a) Case 1 and (b) Case 2.

Table 5. Effect of PCM double layers (10 mm) on energy saving for four regions.

	PCM	Heating/Cooling Energy Saving (Wh/m ²)		Heating and Cooling Energy Saving (Wh/m ²)			
		Heating (Wh/m ²)	Cooling (Wh/m ²)	Energy Saving (Wh/m ²)	Reduction (%)		
Sousse	Single layer	PCM21	2776.46	140.77	2917.23	3.22	
		PCM23	2107.87	246.35	2354.22	2.60	
		PCM25	1161.38	959.39	2120.77	2.34	
		PCM29	32.77	2668.14	2700.91	2.98	
	Double layer (Case 1)	PCM29-PCM21	2512.36	554.99	3067.35	3.39	
		PCM25-PCM21	2236	544.3	2780.3	3.07	
		PCM23-PCM21	2157.28	329.89	2487.17	2.75	
		PCM21-PCM21	2012.97	167.12	2180.09	2.41	
		Double layer (Case 2)	PCM21-PCM29	1828.2	1982.51	3810.71	4.21
			PCM21-PCM25	2074.1	608.87	2682.97	2.96
Bizerte	Single layer	PCM21	2953.44	162.6	3116.04	3.07	
		PCM23	1555.36	390.6	1945.96	1.92	
		PCM25	1130.85	906.57	2037.42	2.01	
		PCM29	82.01	2168.96	2250.97	2.22	
	Double layer (Case 1)	PCM29-PCM21	2150.6	406.79	2557.39	2.52	
		PCM25-PCM21	1980.6	583.17	2563.77	2.52	
		PCM23-PCM21	1884.18	364.32	2248.5	2.21	
		PCM21-PCM21	1724.75	213.3	1938.05	1.91	
		Double layer (Case 2)	PCM21-PCM29	1385.87	1712.64	3098.51	3.06
			PCM21-PCM25	1640.34	672.65	2312.99	2.28
Tabarka	Single layer	PCM21	3067.38	192.55	3259.93	3.58	
		PCM23	1851.81	353.44	2205.25	2.42	
		PCM25	995.52	1005.07	2000.59	2.20	
		PCM29	106.89	1533.01	1639.9	1.80	
	Double layer (Case 1)	PCM29-PCM21	2357.6	345.36	2702.96	2.97	
		PCM25-PCM21	2311.21	547.57	2858.78	3.14	
		PCM23-PCM21	2247.06	379.76	2626.82	2.89	
		PCM21-PCM21	2182.08	230.29	2412.37	2.65	
		Double layer (Case 2)	PCM21-PCM29	1903.66	1280.05	3183.71	3.50
			PCM21-PCM25	2005.68	714.41	2720.09	2.99
Tozeur	Single layer	PCM21	3285.02	189.19	3474.21	3.54	
		PCM23	2977.94	241.46	3219.4	3.28	
		PCM25	1399.59	795.99	2195.58	2.23	
		PCM29	144.85	2249.85	2394.7	2.44	
	Double layer (Case 1)	PCM21-PCM29	2893	606.61	3499.61	3.56	
		PCM21-PCM25	2429.33	484.71	2914.04	2.97	
		PCM23-PCM21	2386.02	296.7	2682.72	2.73	
		PCM21-PCM21	2335.7	187.68	2523.38	2.57	
		Double layer (Case 2)	PCM21-PCM29	2244.52	1670.59	3915.11	3.99
			PCM21-PCM25	2713.79	493.31	3207.1	3.27

The results show that double-layer systems allow for a higher reduction in energy consumption than single-layer systems. This is in good agreement with several previous works [45–47]. In addition, annual heating and cooling energy savings and energy saving rates were calculated for single and double PCM layer systems (Table 5). For all PCMs used as a single layer (10 mm), it can be seen that the annual energy saving is 3.22% in Sousse and 3.54% in Tozeur. Whereas, in the case of double-layer systems, these values become 4.21% and 3.99% for Sousse and Tozeur, respectively. Moreover, the higher energy saving rate value was obtained when using the double-layer PCM29-PCM21 for warm regions and PCM25-PCM21 for cold regions. Hence, the proposed double-PCM layer systems integrated into buildings represent an effective way to improve energy efficiency.

3.5. CO₂ Emission Reduction in the Optimum Cases

As shown previously, the optimal conditions for minimizing the heating and cooling energy requirement vary from one climatic region (city) to another. Therefore, in this section, the energy conserved with these optimized cases for each respective region was calculated and the corresponding CO₂ emission reductions were revealed. The optimum melting temperature for each city was selected; the PCM was located at the best location, and the 40 mm PCM thickness was taken. It was seen that a significant reduction in heating, cooling, and total energy needs can be attained with the optimized integration of PCM. For instance, the total energy need reduction (heating and cooling) reached a value of 37.34%, 26.77%, 34.37%, and 41.61% for Sousse, Bizerte, Tabarka, and Tozeur, respectively (Figure 9). As a result of these reductions in the energy requirement of the building for heating and cooling applications, a considerable amount of CO₂ emission reductions were achieved, corresponding to 34.22%, 25.93%, 34.37%, and 38.74% for Sousse, Bizerte, Tabarka, and Tozeur, respectively (Figure 10). Consequently, the PCM integration with optimized parameters such as melting point, location, and thickness can significantly contribute to energy savings as well as a reduction in CO₂ emissions.

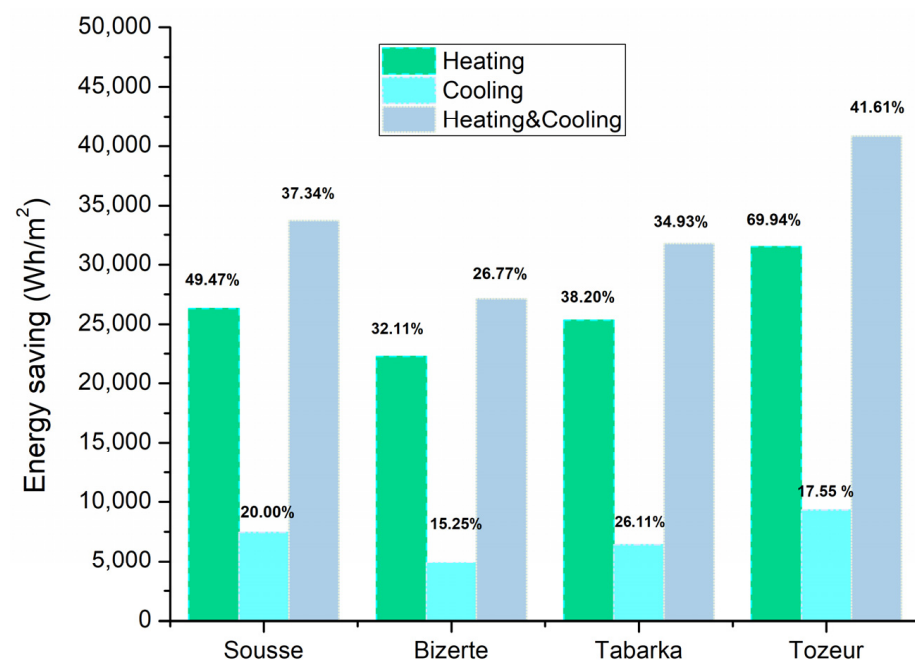


Figure 9. Energy saving in the optimum case.

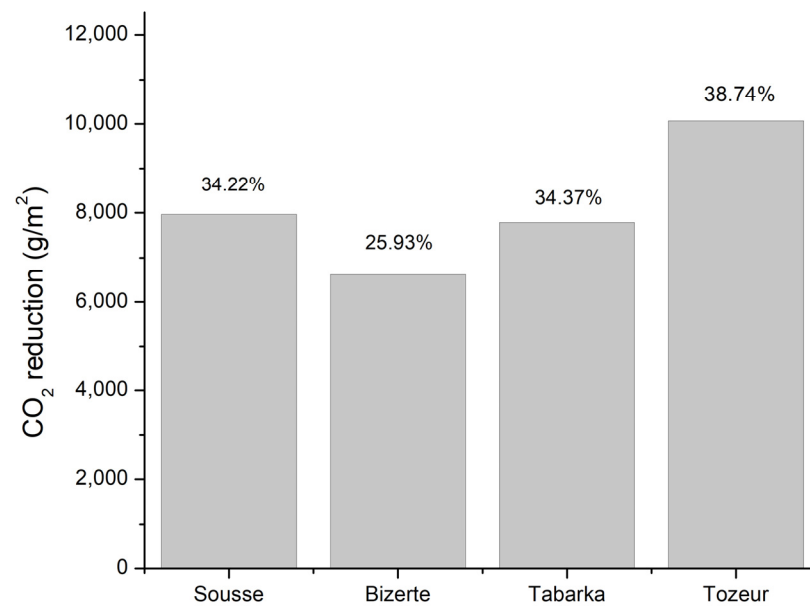


Figure 10. CO₂ emission reduction in the optimum case.

4. Conclusions

The annual energy savings of residential buildings incorporating PCM have been numerically examined in four different climatic regions of Tunisia by considering four cities located in those climates. The potential impacts of PCM melting temperature, location, and thickness were evaluated, along with PCM integration into different building envelopes (roof and external wall). The optimized configuration with respect to the melting point, location, thickness, and building envelope type was found, and the annual energy savings as well as CO₂ emission reductions were explored. Therefore, the following important results were reached in the study:

- Integrating PCM, either in the roof or wall, has a negligible influence on the cooling energy saving.
- The optimal location for the PCM implementation was found to be near the indoor, except for the Sousse region. The percentage energy saving for this optimal location and for the optimal PCM thickness of 40 mm was calculated as 41.61%, 37.34%, 34.93%, and 26.77% for Tozeur, Sousse, Tabarka, and Bizerte, respectively.
- Increasing the PCM thickness in the roof allows an increment in the total annual energy reduction, which varies from 7.97% to 31.42% depending on the climatic region.
- The PCM melting temperature has an important role in energy savings. The best melting temperature was 21 °C, the closest to the set point temperature, which is 21 °C in winter. However, in lower semi-arid regions (Sousse), the melting temperature, which allows the highest reduction in energy need, was 29 °C.
- The use of double-layer PCM with different melting temperatures at different locations represented an alternative for reducing energy consumption. The PCM with a low melting temperature (21 °C) favors heating energy savings, while PCM with a high melting point (29 °C) favors cooling energy savings. Besides, the double-layer systems composed of two different PCM represent a higher efficiency than a PCM single layer mainly in warm and arid regions (Sousse and Tozeur).
- Under optimal conditions of PCM integration in buildings, up to a 38.74% reduction in CO₂ emissions can be achieved in Tozeur.

Author Contributions: S.D.: Conceptualization, Methodology, Software, Investigation, Writing—Original Draft, Visualization, E.T.: Methodology, Software, Formal Analysis, Investigation, Writing—Original Draft, Visualization, O.K.: Formal Analysis, Writing—Original Draft, M.A.: Conceptualization, Formal Analysis, Writing—Review & Editing, Supervision, J.S.: Formal Analysis, Writing—Review & Editing. All authors have read and agreed to the published version of the manuscript.

Funding: This research received no external funding.

Data Availability Statement: Not applicable.

Conflicts of Interest: The authors declare no conflict of interest.

References

1. Al-Rashed, A.; Alnaqi, A.; Alsarraf, J. Usefulness of loading PCM into envelopes in arid climate based on Köppen–Geiger classification—Annual assessment of energy saving and GHG emission reduction. *J. Energy Storage* **2021**, *43*, 103152. [[CrossRef](#)]
2. Beltrán, R.D.; Martínez-Gomez, J. Analysis of phase change materials (PCM) for building wallboards based on the effect of environment. *J. Build. Eng.* **2019**, *24*, 100726. [[CrossRef](#)]
3. Li, Q.; Wang, Y.; Ma, L.; Arıcı, M.; Li, D.; Yıldız, Z.; Zhu, Y. Effect of sunspace and PCM louver combination on the energy saving of rural residences: Case study in a severe cold region of China. *Sustain. Energy Technol. Assess.* **2021**, *45*, 101126. [[CrossRef](#)]
4. Al-Yasiri, Q.; Szabó, M. Incorporation of phase change materials into building envelope for thermal comfort and energy saving: A comprehensive analysis. *J. Build. Eng.* **2021**, *36*, 102122. [[CrossRef](#)]
5. Farouk, N.; El-Rahman, M.A.; Sharifpur, M.; Guo, W. Assessment of CO₂ emissions associated with HVAC system in buildings equipped with phase change materials. *J. Build. Eng.* **2022**, *51*, 104236. [[CrossRef](#)]
6. Wang, X.; Li, W.; Luo, Z.; Wang, K.; Shah, S.P. Design, characteristic and application of phase change materials for sustainable and energy efficient buildings: A review. *Energy Build.* **2022**, *260*, 111923. [[CrossRef](#)]
7. Arumugam, C.; Shaik, S. Air-conditioning cost saving and CO₂ emission reduction prospective of buildings designed with PCM integrated blocks and roofs. *Sustain. Energy Technol. Assess.* **2021**, *48*, 101657. [[CrossRef](#)]
8. Zavrl, E.; Stritih, U. Improved thermal energy storage for nearly zero energy buildings with PCM integration. *Sol. Energy* **2019**, *190*, 420–426.
9. Krarti, M. Multiple-Benefit Analysis of Scaling-Up Building Energy Efficiency Programs: The Case Study of Tunisia. *ASME J. Eng. Sustain. Build. Cities* **2020**, *1*, 1–35. [[CrossRef](#)]
10. Akeiber, H.; Nejat, P.; Majid, M.Z.A.; Wahid, M.A.; Jomehzadeh, F.; Famileh, I.Z.; Calautit, J.K.; Hughes, B.R.; Zaki, S.A. A review on phase change material (PCM) for sustainable passive cooling in building envelopes. *Renew. Sustain. Energy Rev.* **2016**, *60*, 1470–1497. [[CrossRef](#)]
11. Tunçbilek, E.; Arıcı, M.; Krajčák, M.; Li, Y.; Jurčević, M.; Nižetić, S. Impact of nano-enhanced phase change material on thermal performance of building envelope and energy consumption. *Int. J. Energy Res.* **2022**, *46*, 20249–20264. [[CrossRef](#)]
12. Surulivel, T.; Geetha, N.B.; Rajkumar, S. Parametric analysis of thermal behavior of the building with phase change materials for passive cooling. *Energy Sources Part A Recover. Util. Env. Eff.* **2022**, *44*, 5627–5639.
13. Chelliah, A.; Saboor, S.; Ghosh, A.; Kontoleon, K.J. Thermal behaviour analysis and cost-saving opportunities of PCM-integrated terracotta brick buildings. *Adv. Civ. Eng.* **2021**, *2021*, 1–15. [[CrossRef](#)]
14. Li, D.; Yang, R.; Arıcı, M.; Wang, B.; Tunçbilek, E.; Wu, Y.; Liu, C.; Ma, Z.; Ma, Y. Incorporating phase change materials into glazing units for building applications: Current progress and challenges. *Appl. Therm. Eng.* **2022**, *210*, 118374. [[CrossRef](#)]
15. Zhang, S.; Hu, W.; Li, D.; Zhang, C.; Arıcı, M.; Yıldız, Z.; Zhang, X.; Ma, Y. Energy efficiency optimization of PCM and aerogel-filled multiple glazing windows. *Energy* **2021**, *222*, 119916. [[CrossRef](#)]
16. Lu, S.; Xu, B.; Tang, X. Experimental study on double pipe PCM floor heating system under different operation strategies. *Renew. Energy* **2020**, *145*, 1280–1291. [[CrossRef](#)]
17. González, B.; Prieto, M. Radiant heating floors with PCM bands for thermal energy storage: A numerical analysis. *Int. J. Therm. Sci.* **2021**, *162*, 106803. [[CrossRef](#)]
18. Meng, E.; Wang, J.; Yu, H.; Cai, R.; Chen, Y.; Zhou, B. Experimental study of the thermal protection performance of the high reflectivity-phase change material (PCM) roof in summer. *Build. Environ.* **2019**, *164*, 106381. [[CrossRef](#)]
19. Hu, J.; Yu, X. Adaptive building roof by coupling thermochromic material and phase change material: Energy performance under different climate conditions. *Constr. Build. Mater.* **2020**, *262*, 120481. [[CrossRef](#)]
20. Rathore PK, S.; Shukla, S.K. Potential of macroencapsulated PCM for thermal energy storage in buildings: A comprehensive review. *Constr. Build. Mater.* **2019**, *225*, 723–744. [[CrossRef](#)]
21. Hamidi, Y.; Aketouane, Z.; Malha, M.; Bruneau, D.; Bah, A.; Goiffon, R. Integrating PCM into hollow brick walls: Toward energy conservation in Mediterranean regions. *Energy Build.* **2021**, *248*, 111214. [[CrossRef](#)]
22. Kenzhekhanov, S.; Memon, S.A.; Adilkhanova, I. Quantitative evaluation of thermal performance and energy saving potential of the building integrated with PCM in a subarctic climate. *Energy* **2020**, *192*, 116607. [[CrossRef](#)]
23. Navarro, L.; de Gracia, A.; Castell, A.; Álvarez, S.; Cabeza, L.F. PCM incorporation in a concrete core slab as a thermal storage and supply system: Proof of concept. *Energy Build.* **2015**, *103*, 70–82. [[CrossRef](#)]

24. Royon, L.; Karim, L.; Bontemps, A. Thermal energy storage and release of a new component with PCM for integration in floors for thermal management of buildings. *Energy Build.* **2013**, *63*, 29–35. [[CrossRef](#)]
25. Hu, J.; Yu, X. Thermo and light-responsive building envelope: Energy analysis under different climate conditions. *Sol. Energy* **2019**, *193*, 866–877. [[CrossRef](#)]
26. Kumar, S.; Sheeja, R.; Jospher, A.J.; Krishnan, G.S.; Chandrasekar; AroulRaj, A. Energy-saving potential of a passive cooling system for thermal energy management of a residential building in Jaipur City, India. *Mater. Today: Proc.* **2020**, *43*, 1471–1477. [[CrossRef](#)]
27. Mechouet, A.; Oualim, E.M.; Mouhib, T. Effect of mechanical ventilation on the improvement of the thermal performance of PCM-incorporated double external walls: A numerical investigation under different climatic conditions in Morocco. *J. Energy Storage* **2021**, *38*, 102495. [[CrossRef](#)]
28. Hagenau, M.; Jradi, M. Dynamic modeling and performance evaluation of building envelope enhanced with phase change material under Danish conditions. *J. Energy Storage* **2020**, *30*, 101536. [[CrossRef](#)]
29. Fateh, A.; Borelli, D.; Weindlader, H.; Devia, F. Cardinal orientation and melting temperature effects for PCM-enhanced light-walls in different climates. *Sustain. Cities Soc.* **2019**, *51*, 101766. [[CrossRef](#)]
30. Lee, K.O.; Medina, M.A.; Sun, X. Development and verification of an EnergyPlus-based algorithm to predict heat transfer through building walls integrated with phase change materials. *J. Build. Phys.* **2016**, *40*, 77–95. [[CrossRef](#)]
31. Tabares-Velasco, P.C.; Christensen, C.; Bianchi, M. Verification and validation of EnergyPlus phase change material model for opaque wall assemblies. *Build. Environ.* **2012**, *54*, 186–196. [[CrossRef](#)]
32. Kuznik, F.; Virgone, J. Experimental assessment of a phase change material for wall building use. *Appl. Energy* **2009**, *86*, 2038–2046. [[CrossRef](#)]
33. Pedersen, C.O. Advanced zone simulation in EnergyPlus: Incorporation of variable properties and phase change material (PCM) capability. In Proceedings of the Building Simulation, Beijing, China, 15 September 2007; pp. 1341–1345.
34. Nghana, B.; Tariku, F. Phase change material's (PCM) impacts on the energy performance and thermal comfort of buildings in a mild climate. *Build. Environ.* **2016**, *99*, 221–238. [[CrossRef](#)]
35. Kottek, M.; Grieser, J.; Beck, C.; Rudolf, B.; Rubel, F. World map of the Köppen-Geiger climate classification updated. *Meteorol. Z.* **2006**, *15*, 259–263. [[CrossRef](#)]
36. National Institute of Meteorology of Tunisia. Available online: <https://www.meteo.tn/en/> (accessed on 15 May 2022).
37. Available online: http://re.jrc.ec.europa.eu/pvg_tools/en/tools.html#HR (accessed on 15 May 2022).
38. Znouda, E.; Ghrab-Morcos, N.; Hadj-Alouane, A. Un algorithme génétique pour l'optimisation énergétique et économique des bâtiments méditerranéens. In Proceedings of the 6ème conférence Francophone de MOdélisation et SIMulation–MOSIM, Rabat, Morocco, 1 January 2006; Volume 6.
39. Saffari, M.; de Gracia, A.; Fernández, C.; Cabeza, L.F. Simulation-based optimization of PCM melting temperature to improve the energy performance in buildings. *Appl. Energy* **2017**, *202*, 420–434. [[CrossRef](#)]
40. Qu, Y.; Zhou, D.; Xue, F.; Cui, L. Multi-factor analysis on thermal comfort and energy saving potential for PCM-integrated buildings in summer. *Energy Build.* **2021**, *241*, 110966. [[CrossRef](#)]
41. Sovetova, M.; Memon, S.A.; Kim, J. Thermal performance and energy efficiency of building integrated with PCMs in hot desert climate region. *Sol. Energy* **2019**, *189*, 357–371. [[CrossRef](#)]
42. Zhang, Y.; Lin, K.; Jiang, Y.; Zhou, G. Thermal storage and nonlinear heat-transfer characteristics of PCM wallboard. *Energy Build.* **2008**, *40*, 1771–1779. [[CrossRef](#)]
43. Tunçbilek, E.; Arıcı, M.; Bouadila, S.; Wonorahardjo, S. Seasonal and annual performance analysis of PCM-integrated building brick under the climatic conditions of Marmara region. *J. Therm. Anal. Calorim.* **2020**, *141*, 613–624. [[CrossRef](#)]
44. Tong, X.; Xiong, X. A Parametric Investigation on Energy-Saving Effect of Solar Building Based on Double Phase Change Material Layer Wallboard. *Int. J. Photoenergy* **2018**, *2018*, 1829298. [[CrossRef](#)]
45. Cascone, Y.; Capozzoli, A.; Perino, M. Optimisation analysis of PCM-enhanced opaque building envelope components for the energy retrofitting of office buildings in Mediterranean climates. *Appl. Energy* **2018**, *211*, 929–953. [[CrossRef](#)]
46. Zhu, N.; Hu, P.; Xu, L. A simplified dynamic model of double layers shape-stabilized phase change materials wallboards. *Energy Build.* **2013**, *67*, 508–516. [[CrossRef](#)]
47. Louanate, A.; El Otmani, R.; Kandoussi, K.; Boutaous, M. Dynamic modeling and performance assessment of single and double phase change material layer-integrated buildings in Mediterranean climate zone. *J. Build. Phys.* **2021**, *44*, 461–478. [[CrossRef](#)]

Disclaimer/Publisher's Note: The statements, opinions and data contained in all publications are solely those of the individual author(s) and contributor(s) and not of MDPI and/or the editor(s). MDPI and/or the editor(s) disclaim responsibility for any injury to people or property resulting from any ideas, methods, instructions or products referred to in the content.